Inorganic Chemistry

ARTICLE

pubs.acs.org/IC

Fluorescent Zinc(II) Complex Exhibiting "*On-Off-On*" Switching Toward Cu^{2+} and Ag^{+} Ions

Rampal Pandey,[†] Prashant Kumar,[†] Ashish Kumar Singh,[†] Mohammad Shahid,[†] Pei-zhou Li,[‡] Sanjay Kumar Singh,[‡] Qiang Xu,[‡] Arvind Misra,[†] and Daya Shankar Pandey*[,†]

[†]Department of Chemistry, Faculty of Science, Banaras Hindu University, Varanasi -221 005 (U.P.), India

[‡]National Institute of Advanced Industrial Science and Technology (AIST), 1-8-31 Midorigaoka, Ikeda, Osaka 563-8577, Japan

Supporting Information

ABSTRACT: Binuclear zinc(II) and copper(II) complexes based on a new Schiff base ligand *N,N′*-bis(2-hydroxybenzilidene)-2,4,6-trimethylbenzene-1,3-diamine (H_2L) have been synthesized. The ligand H_2L and complexes under investigation have been characterized by elemental analyses, spectral (FT-IR, ^1H, ^{13}C NMR, ESI-MS, electronic absorption, emission), and electrochemical studies. The structures of H_2L and complexes $[\{Zn(C_{23}H_{18}N_2O_2)\}_2]$ (**1**) and $[\{Cu(C_{23}H_{18}N_2O_2)\}_2]\cdot H_2O$ (**2**) have been determined crystallographically. Selective "*On-Off-On*" switching behavior of the fluorescent complex **1** has been studied. The fluorescence intensity of **1** quenches (*turns-off*) upon addition of Cu^{2+}, while enhances (*turns-on*) in the presence of Ag^{+} ions. The mechanisms of "*On-Off-On*" signaling have been supported by ^1H NMR, ESI-MS, electronic absorption, and emission spectral studies. Job's plot analysis supported 1:1 and 1:2 stoichiometries for Cu^{2+} and Ag^{+} ions, respectively. Association and quenching constants have been estimated by the Benesi−Hildebrand method and Stern−Volmer plot. Moreover, **1** mimics a molecular keypad lock that follows correct chemical input order to give maximum output signal.

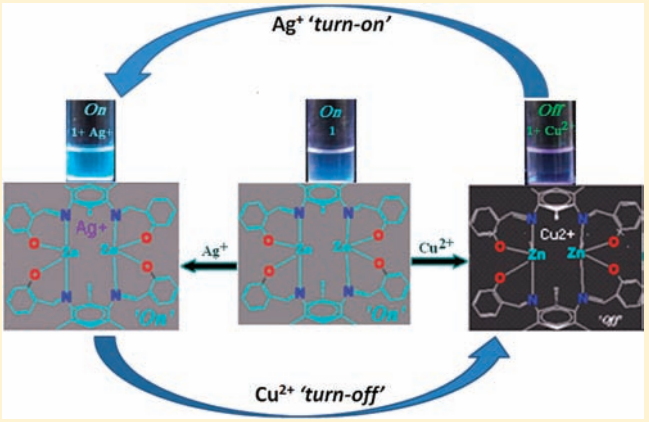

INTRODUCTION

Fluorescent sensing for selective detection of heavy and transition metal (HTM) ions has drawn considerable current attention owing to its high sensitivity and simplicity.[1] The synthesis of biologically and environmentally important HTM ion sensors is interesting, since it can easily undergo chelation in organic media. However, because of a strong hydration factor, most of these have limitations to aqueous environment.[2] In this context, metal ion sensors based on metal−ligand coordination or chemical reactions have been developed.[3] The syntheses of sensors capable of efficient sensing and detection of multiple analytes is challenging.[3] It is well documented that copper acts as a catalytic cofactor for a variety of metalloenzymes, and at the same time, because of widespread applications, it is an important metal pollutant.[4] Likewise, complexes based on silver find applications in medicine and agriculture; however, its prolonged use leads to irreversible darkening of the skin and mucous membrane.[5] Therefore, highly selective and sensitive fluorescent sensors for Cu^{2+} and Ag^{+} ions have been developed.[6] Although most of the HTM ions act as fluorescence quenchers,[3] the emission performance of their complexes strongly depends on the nature of ligand and the structure of resulting compounds. In search of HTM ion sensors, reseachers have synthesized numerous compounds containing salicylaldiminato Schiff bases, which act as blue emitters and find potential applications in various areas.[7] However, binuclear metallacycles based on salen framework exhibiting "*On-Off-On*" switchability toward HTM ions have scarcely been investigated.[8]

Molecular devices based on chemical systems may be employed in the construction of molecular logic networks within a single molecule in vivo or in nano spaces.[9] Generally, in a keypad lock system the output signal depends on the correct order of input signals; therefore, a molecular device that is capable of distinguishing different chemical sequences might be advantageous over simple molecular logic gates.[10] To date, only a few systems have been devised that can selectively and reversibly recognize HTM ions by emitting distinct signals leading to their application as molecular logic gates.[10] With the objective of developing an HTM ion sensor applicable under aqueous conditions, we have synthesized a binuclear zinc(II) complex $[\{Zn(C_{23}H_{18}N_2O_2)\}_2]$ (**1**) based on *N,N′*-bis(2-hydroxybenzilidene)-2,4,6-trimethyl-benzene-1,3-diamine. It has been demonstrated that the present system serves as a fluorescent probe under aqueous conditions (H_2O/MeCN 7:3, v/v and in Tris-HCl buffer system,

Received: May 25, 2010
Published: March 11, 2011

dx.doi.org/10.1021/ic1018086 | *Inorg. Chem.* 2011, 50, 3189–3197

Table 1. Crystal Data and Refinement Parameters for H_2L, 1, and 2

	H_2L	1	2
empirical formula	$C_{23}H_{42}N_2O_2$	$C_{46}H_{40}N_4O_4Zn_2$	$C_{46}H_{40}N_4O_4Cu_2.H_2O$
FW	358.43	843.61	857.96
cryst. syst.	orthorhombic	monoclinic	monoclinic
space group	$P2_12_12_1$	$P2_1/n$	$P2_1/n$
a (Å)	7.0939(14)	10.536(2)	8.2097(16)
b (Å)	12.542(3)	15.095(3)	17.960(4)
c (Å)	21.535(4)	13.134(3)	14.016(3)
β (deg)	90	111.13(3)	103.09(3)
volume (Å^3)	1916.1(7)	1948.4(7)	2013.0(7)
color and habit	yellow, block	white, block	black, block
Z	4	4	4
density calcd. (gcm^{-3})	1.242	1.438	1.445
abs. coeff. (mm^{-1})	0.080	1.281	1.112
F(000)	760	872	908
cryst. size (mm^3)	0.60 × 0.32 × 0.30	0.09 × 0.08 × 0.07	0.36 × 0.32 × 0.30
θ range (deg)	3.02 to 27.48	3.17 to 27.43	2.98 to 27.47
reflns collected	18783	17659	18464
ind. reflns	4381	4410	4598
	[R_{int} = 0.0614]	[R_{int} = 0.112]	[R_{int} = 0.134]
reflns/restraint/params	4381/0/250	4410/0/257	4598/3/273
reflns obs.[$I > 2\sigma(I)$]	2435	2180	2225
goodness-of-fit on F^2	1.025	1.070	1.050
final R ind [$I > 2\sigma(I)$]	R1 = 0.0478	R1 = 0.0624	R1 = 0.1005
	wR2 = 0.0875	wR2 = 0.0993	wR2 = 0.1364
R indices (all data)	R1 = 0.1102	R1 = 0.1602	R1 = 0.2012
	wR2 = 0.1094	wR2 = 0.1432	wR2 = 0.1686

pH ~7.0) for selective detection of Cu^{2+}/Ag^+ ions. Through this work, we present the first report dealing with a dimeric zinc complex [{Zn($C_{23}H_{18}N_2O_2$)}$_2$] acting as a fluorescent probe for selective detection of Cu^{2+}/Ag^+ ions under aqueous conditions and a molecular keypad lock through reversible "*On-Off-On*" switching with distinct signals in the presence of these ions.

EXPERIMENTAL SECTION

General Information and Materials. The reagents and solvents were procured from commercial sources. Solvents were dried and distilled following standard literature procedures.[11] Elemental analyses for C, H, and N were performed on a CE-440 Elemental Analyzer. Infrared and electronic absorption spectra were acquired on a Varian 3300 FT-IR and Shimadzu UV-1601 spectrophotometers, respectively. ^{1}H (300 MHz) and ^{13}C (75.45 MHz) NMR spectra were obtained on a JEOL AL300 FT-NMR spectrometer using tetramethylsilane (TMS) as an internal reference. Fluorescence spectra were recorded on a Varian Cary Eclipse Fluorescence spectrophotometer using Tris-HCl buffer [pH 7−8; water, acetonitrile (7:3)] at room temperature. Electrospray ionization mass spectrometry (ESI-MS) were obtained on a THERMO Finningan LCQ Advantage Max ion trap mass spectrometer. The samples (10 μL) were dissolved in dichloromethane/acetonitrile (3:7, v/v) and introduced into the ESI source through a Finningan surveyor auto sampler. The mobile phase MeOH/MeCN (90:10): H_2O flowed at a rate of 250 μL/min. The ion spray voltage was set at 5.3 KV and capillary voltage at 34 V. The MS scan run up to 2.5 min, and spectra print outs were averaged of over 10 scans. Cyclic voltammetric measurements were performed on a CHI 620c electrochemical analyzer at room temperature. The experiments were made in an airtight single compartment cell using platinum wire as the counter electrode, a glassy carbon working electrode, and Ag/Ag^+ reference electrode.

Preparation of *N,N′*-bis(2-hydroxybenzilidene)-2,4,6-trimethylbenzene-1,3-diamine (H_2L). A methanolic solution (10 mL) of 2,4,6-trimethylbenzene-1,3-diamine (0.751 g, 5.0 mmol) was added to a solution of salicylaldehyde (1.06 mL, 10.0 mmol) in methanol (5 mL), and contents of the flask were heated under reflux for 10 h. After cooling to room temperature it gave yellowish thick oil which upon addition of methanol afforded yellow solid. Recrystallization from dichloromethane/methanol (1:4) gave the desired product as yellow crystals. Yield (1.250 g; 70%). Anal. Calcd. [$C_{23}H_{22}N_2O_2$]: C 77.51, H 5.66, N 7.86%; Found: C 77.43, H 5.62, N 7.82%. ^{1}H NMR ($CDCl_3$, δ_H ppm): 13.02 (s, 2H, O*H*), 8.32 (s, 2H), 7.33−7.40 (m, 4H), 6.95−7.06 (m, 4H), 6.92 (s, 1H), 2.18 (s, 6H), 2.04 (s, 3H). ^{13}C NMR ($CDCl_3$, δ_C ppm): 167.1, 161.17, 146.8, 133.2, 132.4, 132.2, 130.0, 124.7, 119.2, 119.0, 118.7, 117.3, 18.2, 14.00. ESI-MS (m/z): 359.20 [$(M+1)^+$, 100%], 360.20 [$(M+2)^+$, 60%]. IR (KBr pellets, cm^{-1}): 460 (w), 639 (w), 753 (s), 814 (m), 902 (w), 984 (w), 1082 (m), 1147 (w), 1189 (m), 1275 (s), 1403 (m), 1461 (s), 1572 (s), 1621 (vs), 2926 (w), 2976 (w), 3053 (w), 3450 (w). UV−vis. (CH_2Cl_2: MeCN, λ_{max}, nm, ε M^{-1} cm^{-1}): 332 (3.83 × 10^4), 266 (3.04 × 10^4).

Preparation of [{Zn($C_{23}H_{18}N_2O_2$)}$_2$] (1). To an alkaline solution of L^{2-} [prepared by dissolving H_2L (0.358 g, 1.0 mmol) in MeOH (15 mL) and adding KOH (0.112 g, 2.0 mmol) under stirring conditions over half an hour], $Zn(NO_3)_2 \cdot 6H_2O$ (0.594 g, 2.0 mmol) dissolved in MeOH (10 mL) was added dropwise and stirred at room temperature for 1 h. Slowly a white precipitate separated, which was collected by filtration washed with methanol and diethyl ether. Slow diffusion of diethyl ether over a dichloromethane solution of the complex afforded white block shaped crystals in a couple of days. Yield (0.638 g; 76%). Anal. Calcd. [$C_{46}H_{40}Zn_2N_4O_4$]: C 65.49, H 4.78, N 6.64%; Found:

dx.doi.org/10.1021/ic1018086 |*Inorg. Chem.* 2011, 50, 3189–3197

C 65.50, H 4.80, N 6.66%. ^{1}H NMR ($CDCl_3$, δ_H ppm): 7.89 (s, 4H), 7.36 (t, J_1 = 6.9 Hz, J_2 = 7.2 Hz, 4H), 7.04 (d, J = 7.5 Hz, 4H), 6.93 (d, J = 8.4 Hz, 4H), 6.85 (s, 2H), 6.60 (t, J_1 = 7.2 Hz, J_2 = 7.5 Hz, 4H), 2.30 (s, 6H), 1.5 (s, 12H). ^{13}C NMR ($CDCl_3$, δ_C ppm): 174.4, 171.8, 146.5, 136.3, 129.9, 129.5, 124.5, 123.7, 117.8, 114.9, 18.2, 13.00. ESI-MS (m/z): 843.3 [$(M)^+$, 12%], 847.2 [$(M+4)^+$, 10%], 359.3 [$(L+1)^+$, 100%]. IR (KBr pellets, cm^{-1}): 482 (w), 648 (vw), 753 (s), 860 (vw), 922 (w), 1024 (w), 1084 (m), 1143 (m), 1192 (m), 1326 (s), 1352 (m), 1442 (s), 1532 (s), 1609 (vs), 2924 (w), 3423 (w). UV−vis. (CH_2Cl_2: MeCN, λ_{max} nm, ε M^{-1} cm^{-1}): 398 (0.773×10^5), 328 (0.951×10^5), 278 (2.01×10^5).

Preparation of [{Cu($C_{23}H_{18}N_2O_2$)}$_2$]·H_2O (2). To an alkaline solution of L^{2-} [prepared by dissolving H_2L (0.358 g, 1.0 mmol) and adding KOH (0.112 g, 2.0 mmol) under stirring over half an hour] a methanolic solution (10 mL) of $Cu(NO_3)_2 \cdot 3H_2O$ (0.465 g, 2.0 mmol) was added dropwise and stirred at room temperature for 1 h. Slowly a black precipitate separated, which was collected by filtration, washed with methanol and diethyl ether. Black block shaped crystals were obtained by slow diffusion of diethyl ether to a dichloromethane solution of the complex over a couple of days. Yield: (0.699 g; 82%). Anal. Calcd. for $C_{46}H_{40}Cu_2N_4O_4 \cdot H_2O$: C 64.40, H 4.93, N 6.53; Found: C 64.28, H 4.84, N, 6.49%. ESI-MS (m/z): 841 [$(M+1)^+$, 18%], 359.3 [$(L+1)^+$, 100%]. IR (KBr pellets, cm^{-1}): 480 (w), 592 (vw), 753 (s), 831 (vw), 916 (w), 1031 (w), 1090 (m), 1148 (m), 1193 (m), 1320 (s), 1387 (m), 1441 (s), 1531 (s), 1606 (vs), 2915 (w), 3408 (w). UV−vis. (CH_2Cl_2, λ_{max} nm, ε M^{-1} cm^{-1}): 390 (0.871×10^5), 326 (1.01×10^5), 277 (2.08×10^5).

Preparation of [{Zn($C_{23}H_{18}N_2O_2$)}$_2$]$_2$·[Cu]$_2$ (3). To a solution of **1** (0.843 g, 1.0 mmol) in acetonitrile (10 mL), $Cu(NO_3)_2 \cdot 3H_2O$ (1.161 g, 5.0 mmol) dissolved in water (10 mL) was added dropwise and stirred at room temperature for 2 h, whereupon the yellowish green solution turned brown. It was stirred for an additional 4−5 h to ensure that its brown color remained unchanged. The resulting solution was completely evaporated and product dried under vacuum. Product yield and elemental analyses for **3** could not be estimated because of the presence of an excess of paramagnetic $Cu(NO_3)_2 \cdot 3H_2O$. ^{1}H NMR ($CDCl_3$, δ_H ppm): 11.01 (s, 8H), 9.90 (s, 8H), 8.32 (s, 4H), 7.57−7.53 (m, 8H), 7.32−7.23 (m, 8H), 7.02−6.98 (m, 8H), 2.18 (s, 12H), 2.02 (s, 24H). ESI-MS (m/z): 847 [$(\mathbf{1}+4)^+$, 16%], 359.3 [$(L+1)^+$, 16%]. IR (KBr pellets, cm^{-1}): 482 (w), 648 (vw), 759 (s), 860 (vw), 922 (w), 1024 (w), 1084 (m), 1153 (m), 1203 (m), 1283 (s), 1383 (m), 1469 (s), 1546 (s), 1606 (vs), 2929 (w), 3423 (w). UV−vis. (CH_2Cl_2: MeCN, λ_{max} nm, ε M^{-1} cm^{-1}): 357 (1.73×10^5), 269 (3.01×10^5).

Preparation of [{Zn($C_{23}H_{18}N_2O_2$)}$_2$]·[Ag]$_2$ (4). To a solution of **1** (0.841 g, 1.0 mmol) in acetonitrile (10 mL) an aqueous solution (10 mL) of $AgNO_3$ (0.849 g, 5.0 mmol) was added dropwise and stirred at room temperature for 2 h. It was stirred for an additional 4−5 h to ensure that its yellowish green color remains unchanged. The resulting solution was completely evaporated, and the product air-dried. Product yield and elemental analyses for **4** could not be estimated because of the presence of an excess of $AgNO_3$. ^{1}H NMR ($CDCl_3$, δ_H ppm): 11.43 (s, 4H), 8.33 (s, 4H), 7.43−7.33 (m, 4H), 7.06−7.01 (m, 2H), 6.98−6.92 (m, 2H), 6.85 (s, 2H), 6.62−6.57 (t, J_1 = 7.5 Hz, J_2 = 7.2 Hz, 4H), 2.30 (s, 6H), 2.18 (s, 12H). ESI-MS (m/z): 845 [$(\mathbf{1}+2)^+$, 15%], 847 [$(\mathbf{1}+4)^+$, 12%], 360.6 [$(L+2)^+$, 8%], 188 [{$Ag(NO_3)$ (H_2O)}$^+$, 100%]. IR (KBr pellets, cm^{-1}): 482 (w), 648 (vw), 756 (s), 860 (vw), 920 (w), 1028 (w), 1081 (m), 1146 (m), 1190 (m), 1328 (s), 1382 (s), 1451 (s), 1537 (s), 1607 (vs), 2924 (w), 3423 (w). UV−vis. (CH_2Cl_2: MeCN, λ_{max} nm, ε M^{-1} cm^{-1}): 398 (0.773×10^5), 328 (0.951×10^5), 278 (2.01×10^5).

Crystallography. The structures of H_2L and binuclear complexes **1** and **2** have been determined crystallographically. The Oak Ridge thermal-ellipsoid plot (ORTEP) views along with the atom numbering scheme are depicted in Figure 2(a−c). Important crystallographic data and selected geometrical parameters are summarized in Table 1 and Supporting Information, Table S1, respectively. Preliminary data on space group and unit cell dimensions as well as intensity data were collected on a R-AXIS RAPID II diffractometer using graphite monochromatized Mo−Kα radiation (λ = 0.71073 Å) at room temperature. The structures were solved by direct methods (SHELXS 97) and refined by full-matrix least-squares on F^2 (SHELX 97).[12] Non-hydrogen atoms were refined anisotropically. All the hydrogen atoms were geometrically fixed and refined using a riding model. The PLATON computer program was used for analyzing the interaction and stacking distances.[13] Cambridge Crystallographic Data Centre (CCDC) No.'s CCDC-743409 (H_2L), -743411 (**1**), -743410 (**2**) provide access to the supplementary crystallographic data for this paper.

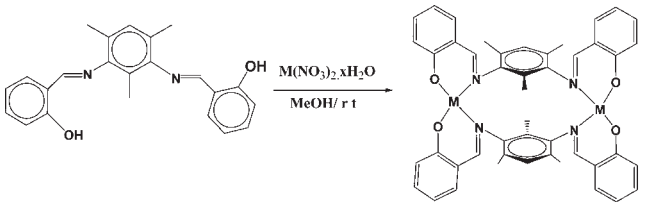

Figure 1. Formation of the complexes **1** and **2**.

Electrochemical Studies. Redox properties of H_2L, **1**, and **2** in the potential range +2.0 to −2.0 V vs Ag/AgCl were followed by cyclic voltammetry in CH_2Cl_2 containing 0.1 M tetrabutylammonium perchlorate as the supporting electrolyte.

UV−vis and Fluorescence Studies. The stock solution of **1** (1.0×10^{-5} M) for electronic absorption and emission spectral studies was prepared using spectroscopic grade MeCN-H_2O (3:7, v/v) in 0.01 M Tris-HCl buffer. The solutions of alkali- and alkaline earth metal ions, first row transition metals, and other cations, namely, Na^+, K^+, Ca^{2+}, Mg^{2+}, Mn^{2+}, Fe^{2+}, Fe^{3+}, Co^{2+}, Ni^{2+}, Cu^{2+}, Zn^{2+}, Ag^+, Cd^{2+}, and Hg^{2+} were prepared by dissolving nitrate salts in triple distilled water (1×10^{-2} M). In the titration studies 3.0 mL solution of **1** (1.0×10^{-5} M) was taken in a quartz cell of 1 cm path length, and solutions of the metal ions were added gradually to the cell.

RESULTS AND DISCUSSION

Synthesis and Characterization. The ligand *N,N′*-bis(2-hydroxybenzilidene)-2,4,6-trimethylbenzene-1,3-diamine (H_2L) was prepared by condensation of 2,4,6-trimethyl-benzene-1,3-diamine and salicylaldehyde (1:2) in methanol under refluxing conditions. Initially an oily product was obtained, which upon addition of dry methanol afforded yellow crystalline compound. Deprotonated H_2L reacted with the hydrated metal nitrates $Zn(NO_3)_2 \cdot 6H_2O$ and $Cu(NO_3)_2 \cdot 3H_2O$ (1:2) to afford binuclear complexes **1** and **2** in reasonably good yields. A simple scheme showing the synthesis of complexes is depicted in Figure 1. The complexes **1** and **2** were characterized by analytical, spectral (IR, NMR, UV−vis, emission, ESI-MS), and electrochemical studies. Crystal structures of **1** and **2** have been authenticated by single crystal X-ray diffraction analyses.

^{1}H NMR spectrum of H_2L is expected to exhibit singlets associated with phenolic and aldimine protons in the downfield side, multiplets corresponding to phenolic ring protons in aromatic region, and resonances due to methyl protons in the highfield side. Expectedly, in $CDCl_3$ it displayed singlets at δ 13.02 and 8.32 ppm assignable to *-OH* and *-CH=N-* protons, respectively. Multiplets at δ 7.33−7.40 and 6.95−7.06 ppm have been assigned to phenolic ring protons while, singlets at δ 2.18 and 2.04 ppm to the methyl protons of 1,3,5-trimethylphenyl ring

dx.doi.org/10.1021/ic1018086 |*Inorg. Chem.* 2011, 50, 3189–3197

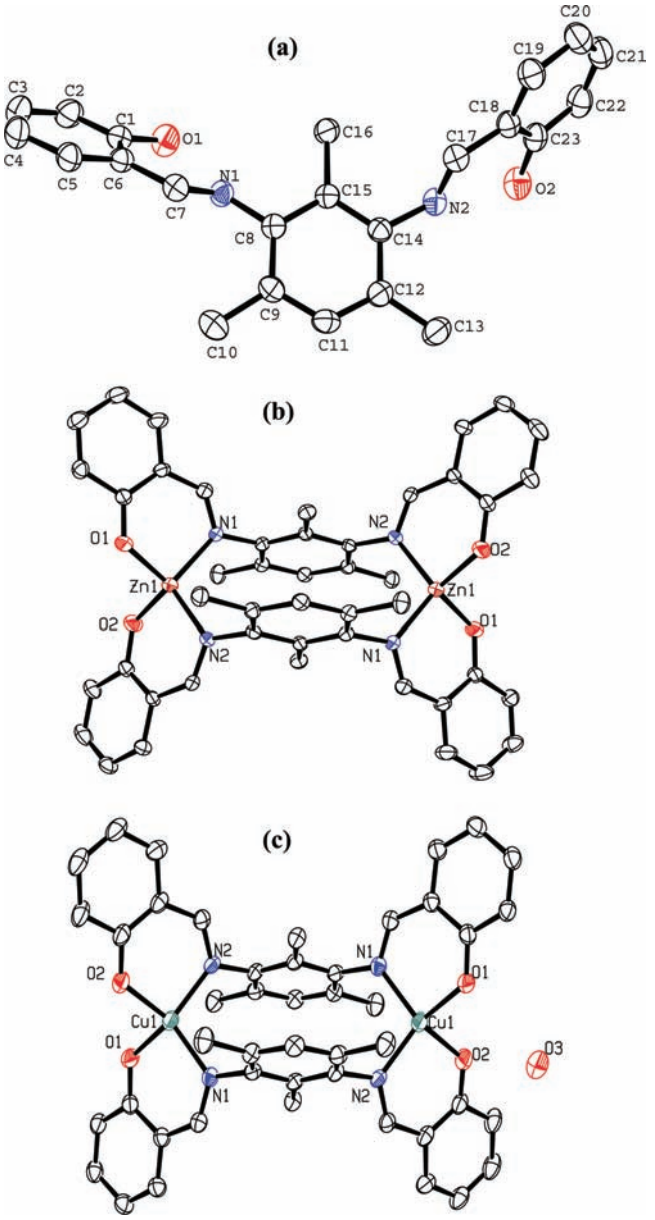

Figure 2. ORTEP views of (a) H_2L, (b) complex **1**, and (c) **2** at 50% thermal probability.

(Supporting Information, Figure S1). The position and integrated intensity of various signals strongly supported the formulation of H_2L wherein, *N,O*-donor sites are *trans-* disposed (Figure 2a). Upon complexation with the metal centers (Zn/Cu) in binuclear metallacycles **1** and **2**, it adopted *cis-* position which has been confirmed by spectral and structural studies. The ligand H_2L crystallizes in orthorhombic space group $P2_12_12_1$. The crystal structure of H_2L exhibited the linkage of 1,3,5-trimethylphenyl ring through phenolato imine group and planarity of phenolato imine and mesitylene rings. Donor sites presented by C17−N2 and C7−N1 are arranged in such a way that they can maintain a minimum distance for intramolecular O−H···N hydrogen bonding between N1···H1−O1 and N2···H2−O2. The bond distances C7−N1 and C17−N2 are 1.280 Å and 1.279 Å, respectively.

Crystal Structure of the Complexes. The complexes **1** and **2** crystallize in the monoclinic system and $P2_1/n$ space group. Crystal structure determination revealed that in cetrosymmetric complexes **1** and **2** deprotonated ligand L^{2-} bridges and chelates two metal(II) centers through phenolato oxygen and imine nitrogen from two different ligands (Figure 2b,c). The zinc(II) centers in **1** are coordinated by phenolato oxygen and imine nitrogen from two ligands leading to a distorted tetrahedral geometry (T_d) about the metal centers with Zn···Zn separation of 7.141 Å.[14] The bond distances Zn−O and Zn−N range from 1.905(4) to 2.016(4) Å [Zn1−N1, 2.016(4); Zn1−N2, 1.999(4); Zn1−O1, 1.907(4); Zn1−O2, 1.905(4)]. Angles between the planes containing O1−Zn−N1 and O2−Zn−N2 are in the range 92.40 to 132.70° [O2−Zn1−N2, 96.02(2); O1−Zn1−N1, 96.07(2)°; O1−Zn1−N2, 122.55(2)° O2−Zn1−N1, 124.29(2)°] while O−Zn−O and N−Zn−N [N2−Zn1−N1, 111.73(2)°; O2−Zn1−O1, 108.44(2)°] are consistent with distorted tetrahedral geometry about the zinc(II) centers.

The Cu−O and Cu−N bond distances in **2** are normal and ranges from 1.88(4) to 1.96(5) Å [Cu1−O2, 1.88(4); Cu1−O1, 1.89(4); Cu1−N2, 1.95(5); Cu1−N1, 1.96(5)].[14] It is evident from the O(N)−Cu−N(O) angles [O2−Cu1−O1, 90.70(2)°; N1−Cu1−N2, 104.00(2)°, O1−Cu1−N1, 94.30(2)°; O1−Cu1−N2, 141.90(2)°; O2−Cu1−N2, 94.62 (2)°, and O2−Cu1−N1, 141.90(2)°] that the coordination geometry about copper(II) centers in **2** are almost halfway between square planar and tetrahedral (Figure 2c). An angle of 51.66° between the planes containing O1−Cu−N1 and O2−Cu−N2 further supported intermediate coordination geometry. Similar observations have been made in other copper(II) complexes.[14] The intermediate geometry may arise from enhancement of geometric ligand strain by the Jahn−Teller effect of T_d copper(II) ions. The metal centers in this complex are separated through an *m*-mesitylene spacer by 7.314 Å that is slightly longer in comparison to other copper(II) complexes.[14] The inter layer centroid-centroid distance between two mesitylene spacers is 3.906 Å. Crystal structure of **2** revealed the presence of a water molecule in its crystal lattice which is involved in strong hydrogen bonding interactions. It leads to hydrogen-bonded array between O3−H···O1 and O3−H···O2 on both the sides of dimeric unit (Supporting Information, Figure S4).

Electrochemical Studies. The cyclic volammogram of H_2L displayed oxidative and reductive responses at +1.0 V and −1.60 V, respectively which may be ascribed to the oxidation of phenolic and reduction of 1,3-diimine moieties.[15] Additional waves in the cyclic voltammogram of **1** and **2** are absent in the positive or negative region. As the zinc(II) center is redox inactive, waves at E_{ox} = +1.092 V and E_{red} = −1.564 V in its cyclic voltammogram (Supporting Information, Figure S5) may be assigned to ligand based oxidation and reduction, respectively.[15] The complex **2** also exhibited an analogous pattern wherein, oxidative and reductive waves appeared at +1.072 and −1.476 V, corresponding to ligand-centered oxidation and reduction, respectively. As compared to H_2L the potentials for **1** and **2** anodically shifted, suggesting electron withdrawing effect in the ligand through coordination to Zn(II)/Cu(II) metal centers upon complexation.

Absorption Spectral Studies. The electronic absorption spectrum of the H_2L displays intense bands at 314 and 258 nm corresponding to n−π^* and π−π^* transitions. In the complex **1** these bands exhibited a red shift and appear at 398 and 278 nm (Figure 3a). The red shift in the position of the absorption bands in comparison to H_2L may be attributed to the formation of a

dx.doi.org/10.1021/ic1018086 |*Inorg. Chem.* 2011, 50, 3189–3197

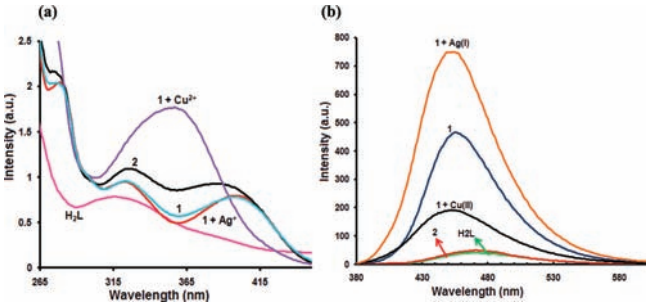

Figure 3. (a) Relative absorption spectra of $\mathbf{H_2L}$, **1**, **2**, **1** + Cu^{2+} (**3**), and **1** + Ag^{+} (**4**) in 0.01 M Tris-HCl buffer (H_2O/acetonitrile, 7:3, v/v; pH 7.0, $c = 1 \times 10^{-5}$ M). (b) Relative fluorescence spectra for H_2L, **1**, **2**, **1** + Cu^{2+} (**3**), and **1** + Ag^{+} (**4**) in Tris- HCl buffer (0.01 M, H_2O/MeCN, 7:3, v/v; pH 7.0, $c = 1 \times 10^{-5}$ M). λ_{ex} = 350 nm, λ_{em}= 458 nm, slit width (5 nm/5 nm, 500 V PMT).

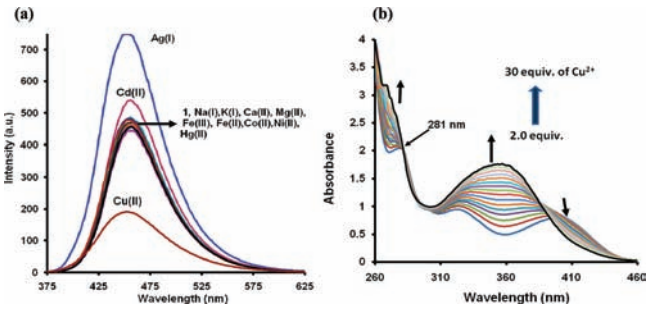

Figure 4. (a) Fluorescence spectra of **1**, upon addition 20.0 equiv. of various metals ions. λ_{ex} = 350 nm, λ_{em}= 458 nm, slit width (5 nm/5 nm, 500 V PMT). (b) Absorption titration spectrum of **1** in the presence of Cu^{2+} ions (2.0−30.0 equiv) in Tris- HCl buffer (0.01 M, H_2O/MeCN, 7:3, v/v; pH 7.0, $c = 1 \times 10^{-5}$ M).

binuclear metallacycle. The stability of **1** was followed in the pH range 6−12 and it was observed that the most stable species exists between pH 7.0−7.4 (Supporting Information, Figure S6). The metal ion interaction studies were performed by addition of nitrate salts of the alkali- and alkaline-earth metal ions, first-row transition metal, and other cations, namely, Na^{+}, K^{+}, Ca^{2+}, Mg^{2+}, Mn^{2+}, Fe^{2+}, Fe^{3+}, Co^{2+}, Ni^{2+}, Cu^{2+}, Zn^{2+}, Ag^{+}, Cd^{2+}, and Hg^{2+} to a solution of **1**. Interstingly, absorption spectra exhibited a significant change in the presence of Cu^{2+}, while other metal ions displayed insignificant changes (Supporting Information, Figure S7; Top).

To have better understanding of the affinity of **1** for Cu^{2+} ions, absorption titration studies were performed by the addition of $Cu(NO_3)_2 \cdot 3H_2O$ (2.0 to 30.0 equiv, Tris-HCl buffer, MeCN/H_2O, 3:7, v/v, pH ∼7.0) to a solution of **1** (Figure 4b). The absorption bands corresponding to **1** disappeared, and an intense band emerged at 357 nm with an isosbestic point at 281 nm. It is quite possible that this band may arise by replacement of the coordinated Zn^{2+} by Cu^{2+} ion. To ascertain this possibility, a strong chelating agent like ethylenediaminetetraacetic acid (EDTA, 10.0 equiv) was added to the solution. Absorption bands associated with **1** restored (Supporting Information, Figure S7; bottom) suggested that the Zn^{2+} has not been replaced by Cu^{2+} ion. It is reasonable to consider that the substitution of Zn^{2+} by Cu^{2+} ion may lead to formation of $[Cu\text{-}L]_2$, which in turn upon addition of EDTA may dissociate to form a more stable complex Cu-EDTA

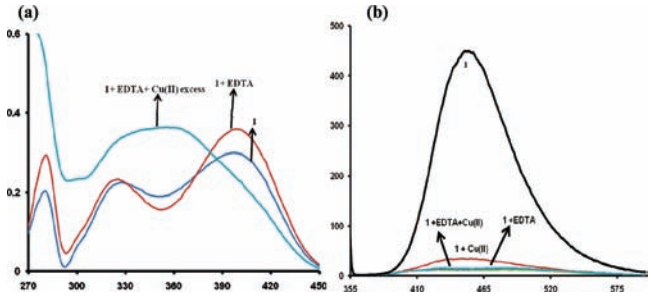

Figure 5. (a) Absorption spectra of **1**, **1** + EDTA (10.0 equiv), and **1** + EDTA + Cu^{2+} (50.0 equiv) upon addition of 20.0 equiv of various metal ions. λ_{ex} = 350 nm, λ_{em}= 458 nm, slit width (5 nm/5 nm, 500 V PMT). (b) Fluorescence titration spectrum of **1** in the presence of Cu^{2+} ions (2.0−30.0 equiv) in Tris-HCl buffer (0.01M, H_2O/MeCN, 7:3, v/v; pH 7.0, $c = 1.0 \times 10^{-5}$ M).

owing to the higher affinity of Cu^{2+} ion for EDTA. On the other hand, addition of EDTA (10 equiv) to a solution of **1** exhibited insignificant changes in the position of absorption bands indicating that the Zn^{2+} is not being liberated from **1** to form a Zn-EDTA complex (Figure 5a). Again, addition of a large excess of Cu^{2+} (60 equiv) to the same solution leads to the emergence of the band at ∼357 nm, suggesting interaction between **1** and Cu^{2+} present in the solution. Further, to ensure that the band at 357 nm is not due to binuclear copper complex formed by substitution of Zn^{2+}, absorption spectra of **2** was acquired in the same solvent system. It displayed transitions at 390, 326, and 277 nm. The presence of a low energy band at 390 nm instead of the one at 357 nm indicated that the observed spectral changes are not due to substitution of Zn^{2+} by Cu^{2+}. It suggested that some sort of interaction is certainly taking place between **1** and Cu^{2+} ions, but is not arising from the substitution of Zn^{2+} by Cu^{2+} ions. A blue shift of ∼30 nm may be attributed to interaction of Cu^{2+} ions probably through imine units of the complex **1**. Job's plot analysis (Supporting Information, Figure S9) further supported 1:1 stoichiometry between **1** and Cu^{2+} ions.

Fluorescence Spectral Studies. The ligand H_2L and complex **2** do not show any noticeable fluorescence upon excitation at 350 nm. Further, H_2L do not show any substantial fluorescence changes in the presence of various metal ions (20.0 equiv) except Zn^{2+} (Figure 3b, Supporting Information, Figure S8; Top). The complex **1** displays weak fluorescence at 458 nm with a Stokes shift of ≈108 nm upon excitation at 350 nm. High fluorescent behavior of **1** may be attributed to the complex formation leading to reduction of PET process.[16] Six-membered chelate ring present in the zinc complex **1** increases rigidity in comparison to H_2L, which in turn, reduces the loss of energy by vibrational decay and enhances the fluorescence intensity by a factor of ∼11.[17] The fluorescence behavior of **1** has also been examined in dichloromethane (DCM), and we found that it produces measurable signal even in nanomolar (nM) range (Supporting Information, Figure S8; bottom). The quantum yield (Φ_F) for H_2L (0.05), **1** (0.65), and **2** (0.06) has been determined with respect to the Zn(salen) (Φ_F = 0.10 in dichloromethane).[18] The quantum yield of the complex **1** is comparable to that of other fluorescent salen based Zn-complexes.[18a−c]

The complex **1** may serve as a potential fluorescent sensor. To demonstrate this behavior nitrate salts of the tested metal ions (H_2O; 20.0 equiv, c = 1×10^{-2} M) were added to a solution of **1** and emission spectral changes monitored. The fluorescence

dx.doi.org/10.1021/ic1018086 |*Inorg. Chem.* 2011, 50, 3189–3197

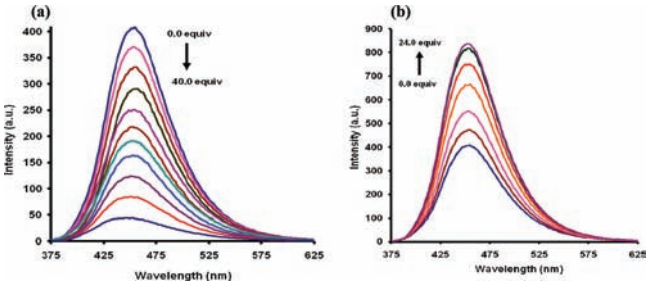

Figure 6. (a) Fluorescence titration spectra upon addition of Cu^{2+} ion (0.0−40.0 equiv) to a solution of **1**; (b) Change in the fluorescence spectra upon addition of Ag^{+} ion (0.0−24.0 equiv) to a solution of **1**. λ_{ex} = 350 nm, λ_{em} = 458 nm, slit width (5 nm/5 nm, 500 V PMT).

quenching/enhancements were observed only upon addition of Cu^{2+}/Ag^{+} ions (Figure 4a and Supporting Information, Figure S9; top). Addition of the Cu^{2+} and Ag^{+} ions (20.0 equiv) displayed ∼60% fluorescence quenching (Figure 4a and 6a), and ∼56% enhancement, respectively (Figure 4a and 6b). Quenching by Cu^{2+} has been investigated by electronic absorption and emission titrations. Addition of Cu^{2+} ion (2.0−40.0 equiv; interval time, 5 min.) leads to the fluorescence quenching ("*turn-off*" ∼89%, Figure 6a), and the quantum yield decreases to 0.005.[18e] To gain deep insight into the mode of quenching by Cu^{2+}, an axcess of EDTA (10.0 equiv) was added to a solution of **1**. The fluorescence due to **1** completely quenched and could not be restored further by additions of Cu^{2+} (40.0 equiv). On the other hand, addition of Cu^{2+} (40.0 equiv) to a solution of **1** leads to the fluorescence quenching, "*turn-off*" (∼90%) which could not be restored by subsequent addition of 10.0 equiv of EDTA (Figure 5b). It suggested that the observed fluorescence quenching is not due to the substitution of Zn^{2+} from **1**. Detailed information about the mode of quenching in the presence of Cu^{2+} has been deduced from Stern−Volmer plot (K_{sv} = 8,500 M^{-1}). A straight line obtained in the S−V plot suggested dynamic quenching (Supporting Information, Figure S10). The association constants (K_a) deduced[22] for 1:1 stoichiometry, based on emission and absorption titration studies are 3.29 and 3.54 log K_a, respectively (Supporting Information, Figure S11). It was further observed that an increase in the time interval for addition of Cu^{2+} leads to insignificant changes in the absorption as well as fluorescence spectral patterns.

Similarly, the fluorescence titration experiments employing Ag^{+} ions (2.0 to 24.0 equiv) display gradual fluorescence enhancement "*turn-on*" (Figure 6b) with an improved quantum yield (0.76).[18f] To ensure that displacement of Zn^{2+} by Ag^{+} ion is not responsible for "*turn-on*" behavior, an unsuccessful attempt was made to isolate the silver complex by direct reaction of $AgNO_3$ with H_2L.[14] As direct reaction of $AgNO_3$ with H_2L does not give a Ag-complex, the possibility of displacement mode can be ruled out. It suggested that the fluorescence enhancement possibly arises from charge transfer through weak interaction between **1** and Ag^{+} ion.[19,23] The Job's plot analysis (Supporting Information, Figure S9) shows 1:2 stoichiometry between **1** and Ag^{+} ion and the association constant (K_a) from a B−H plot based on emission titration studies (Supporting Information, Figure S10) is 8.05 log K_a.[22] Although the color of solutions containing H_2L, **1**, **3**, and **4** under UV light are not significantly different, however, the fluorescence intensity of **1** diminishes and enhances in the presence of Cu^{2+} and Ag^{+} ions, respectively (Figure 8a, inset).

^{1}H NMR Studies. To have clear idea about the mechanism of quenching/enhancement taking place in the presence of Cu^{2+}/Ag^{+} ions, ^{1}H NMR studies were performed on H_2L, **1**, **2**, **1** + Cu^{2+} (**3**), and **1** + Ag^{+} (**4**) (Figure 7). For the sake of clarity shifts in the position of aldimine proton -C*H*=N- (denoted as *H*1) have been followed by ^{1}H NMR spectral studies. The -CH=N- proton of H_2L resonates at δ 8.32 ppm. Upon complexation with the metal center Zn, it exhibited an upfield shift and resonated at δ 7.89 ppm (Figure 7 and Supporting Information, Figure S2; Top). The *H*1 and *H*2 protons of **3** displayed a downfield shift and resonated at 11.01 and 9.90 ppm, respectively (Figure 7 and Supporting Information, Figure S3; Top). The downfield shift in the position of *H*1 and *H*2 suggested that Cu^{2+} is interacting with the -CH=N- moiety (Scheme) in 1:1 stoichiometric ratio.[19a,b] From the crystal structures of **1** and **2** it is clear that the only difference between these complexes lies in their metal center. Therefore, such a large shift in the position of *H*1 and *H*2 protons is not expected if Zn^{2+} is substituted by Cu^{2+}. Further, as expected a well resolved ^{1}H NMR spectrum for **2** could not be obtained because of paramagnetic Cu^{2+} (d^9) ions and ferromagnetic coupling.[14] Interaction of Cu^{2+} with aldimine moieties may subsequently be responsible for metal to ligand charge transfer (MLCT) transitions and quenching.

In comparison to **3**, the -CH=N- protons in **4** exhibited a downfield shift and resonated at δ 11.43 ppm, while the *H*2 proton resonated in the high field side at δ 8.34 ppm (Figure 7 and Supporting Information, Figure S3; Bottom). It suggested that Ag^{+} is interacting more strongly than Cu^{2+} with the -CH=N- moiety, which has further been supported by a higher association constant value (8.05 log K_a) for Ag^{+} ion.[23] It also supported the results from fluorescence titration studies that the addition of 24.0 equiv of Ag^{+} leads to saturation of fluorescence enhancement plot, while 40.0 equiv is required for Cu^{2+}.

Electrospray Mass Spectrometry. The ESI-MS of H_2L displayed a molecular ion peak $[M+1]^+$ (100%) at *m*/*z* 359.2 (Supporting Information, Figure S12; Top). In its mass spectrum **1** displayed peaks associated with $[M]^+$, $[M+4]^+$, and $[L+1]^+$ at *m*/*z* 843.3 (12%), 847.2 (10%), and 359.3 (100%), respectively. The presence of various peaks strongly supported formulation of **1** (Supporting Information, Figure S12; middle). Similarly, **2** displayed molecular ion peak at *m*/*z* 841.2 (18%) alongwith a peak associated with $[L+1]^+$ at *m*/*z* 359.3 (100%) (Supporting Information, Figure S12; bottom). To have an idea about the quenching/enhancement in the presence of Cu^{2+}/Ag^{+} ions, mass spectra of **3** and **4** were acquired. In its MS spectrum **3** exhibited prominent peak at *m*/*z* 847.6 (16%) assignable to $[1+4]^+$ (Supporting Information, Figure S13; top); on the other hand, **4** displayed peaks at *m*/*z* 845 (15%) and 847 (12%) corresponding to $[1+2]^+$ and $[1+4]^+$ (Supporting Information, Figure S13; bottom). The observed ESI-MS spectral patterns for **3** and **4** are quite different from that of **1**. It may be concluded that Cu^{2+} and Ag^{+} ions are interacting with **1** (Supporting Information, Figure S12 and S13). The spectral data are consistent with the conclusions drawn from ^{1}H NMR spectral studies.

On the basis of ^{1}H NMR and ESI-MS spectral studies the probability of displacement of Zn^{2+} from **1** by Cu^{2+}/Ag^{+} has been ruled out. The observed dynamic fluorescence quenching can be accounted by considering two-way charge transfer between aldimine (-C═N-) moiety of **1** and paramagnetic Cu^{2+} ions.[19] Interaction of **1** with Cu^{2+} may lead to the formation of nonfluorescent species by bringing paramagnetic Cu^{2+} close to

dx.doi.org/10.1021/ic1018086 |*Inorg. Chem.* 2011, 50, 3189–3197

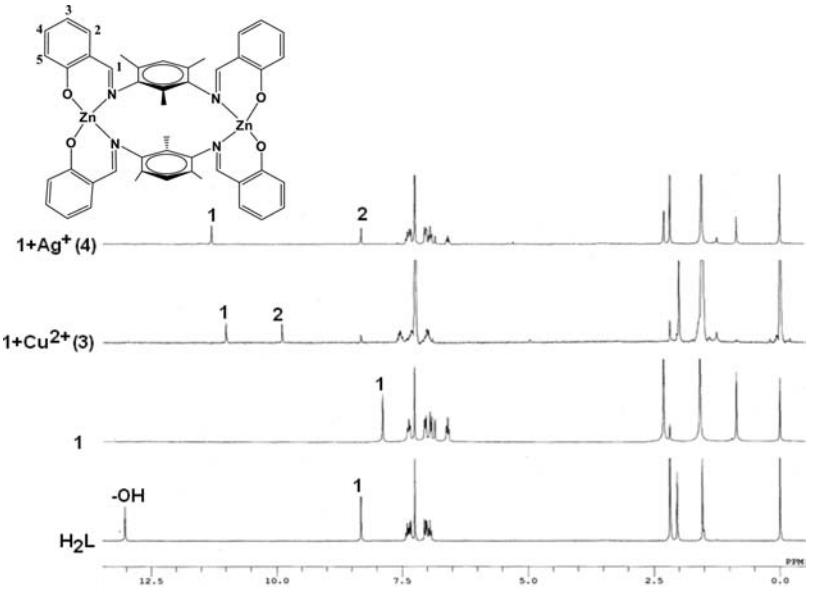

Figure 7. ^{1}H NMR spectrum of H_2L, **1**, **3**, and **4**.

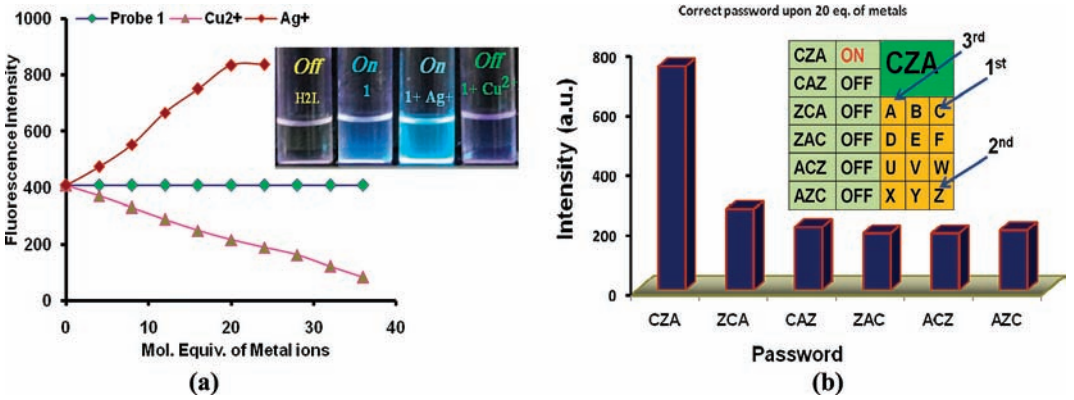

Figure 8. (a) Relative changes in the fluorescence spectra of **1**, upon addition of various equiv of Ag^+ ion (0.0−24.0 equiv) and Cu^{2+} ion (0.0−40.0 equiv); Inset shows fluorescent distinction visible by the naked eye under UV-light irradiation at 254 nm. (b) Output for **1**, corresponding to six possible input combinations at 458 nm. Inset shows a molecular keypad lock generating emission at 458 nm when a correct password, namely, CZA, is entered. Keys C, Z, and A hold the relevant inputs Cu^{2+}, Zn^{2+}, and Ag^+, respectively.

the chromophore with enhanced intersystem crossing.[20] Similarly, observed enhanced fluorescence signal in the presence of Ag^+ may be attributed to one way electron transfer from aldimine (-CH=N-) to diamagnetic Ag^+ ion (d^{10}).[21a−c] Further, interaction of Ag^+ ion with both aldimine and phenolato oxygen atom in 1:2 stoichiometry may result in restricted PET that enhances the fluorescence.[21d,e]

As Molecular Keypad Lock. Recently, Kumar et al.[24c] reported a fluorogenic chemosensor based on a calix[4]arene which acts as an "*On-Off*" reversible switch with chemical inputs of Hg^{2+} and K^+ ions and works as a molecular keypad lock in the presence of F^- ions. On the basis of the findings of Kumar et al and other research groups, it was realized that the present system may also serve as a potential molecular keypad lock system.[10,24] Complex **1** under investigation exhibits reversible fluorescence quenching (*turn-off*)/enhancement (*turn-on*) in the presence of Cu^{2+}/Ag^+ ions, respectively. The reversibility and selectivity of **1** toward Cu^{2+}/Ag^+ ions prompted us to consider the present system as a sequence dependent molecular keypad lock using the Cu^{2+}, Zn^{2+}, and Ag^+ metal ions as three different chemical inputs. It was observed that **1** displayed distinct fluorescence signals corresponding to given chemical input. Inputs in the order Cu^{2+}→Zn^{2+}→Ag^+ provided maximum output whereas Ag^+→Zn^{2+}→Cu^{2+} afforded minimum output (the Zn^{2+} ion was used as an intermediate chemical input because the addition of Zn^{2+} leads to restoration of the fluorescence of **1**). These chemical inputs may be executed in the form of Cu^{2+}, Zn^{2+}, and Ag^+, designated as 'C', 'Z', and 'A', respectively. Among the possible six input combinations, CZA, CAZ, ZAC, ZCA, ACZ, and AZC, the combination CZA gave maximum fluorogenic output, whereas minimum output signaling was displayed by AZC (Figure 8b). The keypad shown in figure 8b (inset) contains various keys, (i.e., A, B, C, D, E, F, U, V, W, X, Y, Z) like that in the electronic keypad (containing A to Z) and follows correct password order (CZA). The mechanism behind the maximum or minimum fluorogenic outputs have been ascribed

dx.doi.org/10.1021/ic1018086 |*Inorg. Chem.* 2011, 50, 3189–3197

to the weak interaction {M-π (-C*H*=N-)} between **1** and Cu^{2+}/Ag^{+} ions. Since, Cu^{2+} and Ag^{+} ions do not displace Zn^{2+} from **1**, the added metal ions (Cu^{2+}/Zn^{2+}/Ag^{+}) weakly interact with **1**. The addition of a particular metal ion (Cu^{2+}/Zn^{2+}/Ag^{+}) dominates over the metal ion present in solution and weakly interacts with **1** thus exhibiting the fluorescence owing to added metal ion. As none of the added metal ions interact with **1** through covalent/coordinate bond, it is possible that the incoming metal ion may interact with **1** replacing the other, as a result complex **1** mimic between three distinct fluorescence states. Such types of chemical systems may be applicable to protect the information at molecular level as it requires correct password entries.[10] Although, a few molecular keypad lock systems are available in literature,[10,24] all these are based on organic molecules whereas the system described in this work is based on a binuclear Zn complex.[25]

CONCLUSIONS

In summary, through this work we have described the synthesis, spectral and structural characterization of binuclear zinc(II) and copper(II) complexes based on a new salen type ligand *N*,*N*′-bis(2-hydroxybenzilidene)-2,4,6-trimethylbenzene-1,3-diamine. The zinc complex displays strong fluorescence, which is measurable even at nanomolar concentrations. It exhibits "*turn-off*" and "*turn-on*" in the presence of Cu^{2+} and Ag^{+} ions in aqueous environment at neutral pH. The "*Off-On*" processes are reversible, and it has been established that they arises from weak interaction between Cu^{2+}/Ag^{+} and -C*H*=N- unit. The observed fluorescence quenching of **1** in the presence of paramagnetic Cu^{2+} has been attributed to interaction of Cu^{2+} with the -CH=N- unit, subsequently metal to ligand charge transfer (MLCT) to the chromofore of **1**. On the other hand, fluorescence enhancement in the presence of Ag^{+} possibly arises from ligand to metal charge transfer (LMCT) between **1** and Ag^{+} (d^{10}). Moreover, **1** can be applied as a molecular keypad lock system which follows correct chemical input order CZA (Cu^{2+}→Zn^{2+}→Ag^{+}) because of reversible "*switch-off*" and "*switch-on*" signaling in the presence of Cu^{2+} and Ag^{+} ions, respectively. The present approach can be further extended to yield a new class of chemosensors with potential applications.

ASSOCIATED CONTENT

Supporting Information. Contains characterization data, UV−vis and emission spectra related to this work, and crystal data in CIF format (CCDC-743409, 743411, 743410) for H_2L, complex **1** and **2**. This material is available free of charge via the Internet at http://pubs.acs.org.

AUTHOR INFORMATION

Corresponding Author

*E-mail: dspbhu@bhu.ac.in. Phone: + 91 542 6702480. Fax: + 91 542 2368174.

ACKNOWLEDGMENT

Thanks are due to the Department of Science and Technology, New Delhi, India for financial assistance through the Scheme SR/S1/IC-15/2006. The authors are also grateful to the National Institute of Advanced Industrial Science and Technology (AIST), Osaka, Japan for extending use of the single-crystal X-ray diffraction facility.

REFERENCES

(1) (a) Nolan, E. M.; Lippard, S. J. *Chem. Rev.* **2008**, *108*, 3443–3480. (b) Que, E. L.; Domaille, D. W.; Chang, C. J. *Chem. Rev.* **2008**, *108*, 1517–1549. (c) Kikuchi, K.; Komatsu, K.; Nagano, T. *Curr. Opin. Chem. Biol.* **2004**, *8*, 182–191. (d) Prodi, L.; Bolletta, F.; Montalti, M.; Zaccheroni, N. *Coord. Chem. Rev.* **2000**, *205*, 59–83. (e) Valeur, B.; Leray, I. *Coord. Chem. Rev.* **2000**, *205*, 3–40. (f) Desvergne, J. P.; Czarnik, A. W. *Chemosensors of Ion and Molecule Recognition*; Kluwer: Dordrecht, The Netherlands, 1997. (g) de Silva, A. P.; Gunaratne, H. Q. N.; Gunnlaugsson, T.; Huxley, A. J. M.; McCoy, C. P.; Rademacher, J. T.; Rice, T. E. *Chem. Rev.* **1997**, *97*, 1515–1566.

(2) (a) Klein, G.; Kaufmann, D.; Schürch, S.; Reymond, J.-L. *Chem. Commun.* **2001**, 561–562. (b) Prodi, L.; Bargossi, C.; Montalti, M.; Zaccheroni, N.; Su, N.; Bradshaw, J. S.; Izatt, R. M.; Savage, P. B. *J. Am. Chem. Soc.* **2000**, *122*, 6769–677.

(3) (a) Domaille, D. W.; Que, E. L.; Chang, C. J. *Nat. Chem. Biol.* **2008**, *4*, 168–175. (b) Royzen, M.; Durandin, A.; Young, V. G., Jr.; Geacintov, N. E.; Canary, J. W. *J. Am. Chem. Soc.* **2006**, *128*, 3854–3855. (c) Zhang, X.; Shiraishi, Y.; Hirai, T. *Org. Lett.* **2007**, *9*, 5039–5042. (d) Ray, D.; Bharadwaj, P. K. *Inorg. Chem.* **2008**, *47*, 2252–2254.

(4) (a) Yardim, M. F.; Budinova, T.; Ekinci, E.; Petrov, N.; Razvigorova, M.; Minkova, V. *Chemosphere* **2003**, *52*, 835–841. (b) Løvstad, R. A. *BioMetals* **2004**, *17*, 111. (c) Barceloux, D. G.; Barceloux, D. J. *Clin. Toxicol.* **1999**, *37*, 217. (d) Sarkar, B. In *Metal ions in biological systems*; Siegel, H., Siegel, A., Eds.; Marcel Dekker: New York, 1981; Vol. 12, pp 233 ff. (e) Que, E. L.; Domaille, D. W.; Chang, C. J. *Chem. Rev.* **2008**, *108*, 1517.

(5) (a) Jung, W. K.; Koo, H. C.; Kim, K. W.; Shin, S.; Kim, S. H.; Park, Y. H. *Appl. Environ. Microbiol.* **2008**, *74*, 2171–2178. (b) Silver, S.; Phung, L. T.; Silver, G. J. *Ind. Microbiol. Biotechnol.* **2006**, *33*, 627–634. (c) Melaiye, A.; Simons, R. S.; Milsted, A.; Pingitore, F.; Wesdemiotis, C.; Tessier, C. A.; Youngs, W. J. *J. Med. Chem.* **2004**, *47*, 973–977. (d) Mozingo, D. W.; McManus, A. T.; Kim, S. H.; Pruitt, B. A. *J. Trauma* **1997**, *42*, 1006–1010. (e) Melaiye, A.; Sun, Z.; Hindi, K.; Milsted, A.; Ely, D.; Reneker, D. H.; Tessier, C. A.; Youngs, W. J. *J. Am. Chem. Soc.* **2005**, *127*, 2285–2291. (f) Butkus, M. A.; Labare, M. P.; Starke, J. A.; Moon, K.; Talbot, M. *Appl. Environ. Microbiol.* **2004**, *70*, 2848–2856. (g) Petering, H. G. *Pharmacol. Ther. A* **1976**, *1*, 127–130. (h) Russell, A. D.; Hugo, W. B. *Prog. Med. Chem.* **1994**, *31*, 351–370.

(6) (a) Amendola, V.; Fabbrizzi, L.; Foti, F.; Licchelli, M.; Mangano, C.; Pallavicini, P.; Poggi, A.; Sacchi, D.; Taglietti, A. *Coord. Chem. Rev.* **2006**, *250*, 273–273. (b) Kramer, R. *Angew. Chem., Int. Ed.* **1998**, *37*, 772–773. (c) Joseph, R.; Ramanujam, B.; Acharya, A.; Rao, C. P. *J. Org. Chem.* **2009**, *74*, 8181–8190.

(7) (a) Sano, Y.; Nisho, Y.; Hamada, H.; Takahashi, T.; Usuki; Shibata, K. *J. Mater. Chem.* **2000**, *10*, 157–161. (b) Natrajan, L. S.; Timmins, P. L.; Lunn, M.; Heath, S. L. *Inorg. Chem.* **2007**, *46*, 10877–10886, and references therein.

(8) de Silva, S. A.; Zavaleta, A.; Allam, D. E. B. O.; Isidor, E. V.; Kashimura, N.; Percarpio., J. M. *Tetrahedron Lett.* **1997**, *38*, 2237–2240.

(9) (a) de Silva, A. P.; James, D. Y.; McKinney, B. O. F.; Pears, D. A.; Weir, S. M. *Nat. Mater.* **2006**, *5*, 787–790. (b) Rinaudo, K.; Bleris, L.; Maddamsetti, R.; Subramanian, S.; Weiss, R.; Beneson, Y. *Nat. Biotechnol.* **2007**, *25*, 795–801.

(10) (a) Margulies, D.; Felder, C. E.; Melman, G.; Shanzer, A. *J. Am. Chem. Soc.* **2007**, *129*, 347–354. (b) Guo, Z.; Zhu, W.; Shen, L.; Tian, H. *Angew. Chem., Int. Ed.* **2007**, *46*, 5549–5553.

(11) Perrin, D. D.; Armango, W. L. F.; Perrin, D. R.; *Purification of Laboratory Chemicals*; Pergamon: Oxford, U.K. 1986.

(12) (a) Sheldrick, G. M. *SHELXL-97, Program for X-ray Crystal Structure Refinement*; Göttingen University: Göttingen, Germany, 1997. (b) Sheldrick, G. M. *SHELXS-97, Program for X-ray Crystal Structure Solution*; Göttingen University: Göttingen, Germany, 1997.

(13) (a) Spek, A. L. *PLATON, A Multipurpose Crystallographic Tools*; Utrecht University: Utrecht, The Netherlands, 2000. (b) Spek, A. L. *Acta Crystallogr., Sect. A* **1990**, *46*, C31–37.

(14) (a) Hernández-Molina, R.; Mederos, A.; Gili, P.; Domínguez, S.; Lloret, F. *J. Chem. Soc., Dalton Trans.* **1997**, 4327–4334. (b) Pardo, E.; Ruiz-García, R.; Lloret, F.; Julve, M.; Cano, J.; Pasàn, J.; Ruiz-Pèrez, C.; Filali, Y.; Chamoreau, L.-M.; Journaux, Y. *Inorg. Chem.* **2007**, *46*, 4504–4514. (c) Palacios, M. A.; Rodríguez-Diéguez, A.; Sironi, A.; Herrera, J. M.; Mota, A. J.; Cano, J.; Colacio, E. *Dalton Trans.* **2009**, 8538–8547.

(15) (a) Yam, V. W-W.; Pui, Y-L; Cheung, K-K *New J. Chem.* **1999**, *23*, 1163–1169. (b) Yam, V. W-W.; Pui, Y.-L.; Cheung, K.-K. *Inorg. Chem.* **2000**, *39*, 5741–5746.

(16) Sreedaran, S.; Bharathi, K. S.; Rahiman, A. K.; Jagadish, L.; Kaviyarasan, V.; Narayanan, V. *Polyhedron* **2008**, *27*, 2931–2938.

(17) (a) Williams, N. J.; Gan, W.; Reibenspies, J. H.; Hancock, R. D. *Inorg. Chem.* **2009**, *48*, 1407–1415. (b) Li, S.-N.; Zhai, Q.-G.; Hu, M.-C.; Jiang, Y.-C. *Inorg. Chim. Acta* **2009**, *362*, 2217–2221. (c) Basak, S.; Sen, S.; Marschner, C.; Baumgartner, J.; Batten, S. R.; Turner, D. R.; Mitra, S. *Polyhedron* **2008**, *27*, 1193–1200.

(18) (a) Deda, M. L.; Ghedini, M.; Aiello, I.; Grisolia, A. *Chem. Lett.* **2004**, *33*, 1060–1061. (b) Wang, P.; Hong, Z.; Xie, Z.; Tong, S.; Wong, O.; Lee, C.-S.; Wong, N.; Hung, L.; Lee, S. *Chem. Commun.* **2003**, 1664–1665. (c) Pucci, D.; Aiello, I.; Bellusci, A.; Crispini, A.; Ghedini, M.; Deda, M. L. *Eur. J. Inorg. Chem.* **2009**, 4274–4281. (d) Xue, L.; Liu, Q.; Jiang, H. *Org. Lett.* **2009**, *11*, 3454–3457. (e) Weng, Y.-Q.; Teng, Y.-L.; Yue, F.; Zhong, Y.-R.; Ye, B.-H. *Inorg. Chem. Commun.* **2007**, *10*, 443–446. (f) Coskun, A.; Akkaya, E. U. *J. Am. Chem. Soc.* **2005**, *127*, 10464–10465.

(19) (a) Stoufer, R. C.; Busch, D. H. *J. Am. Chem. Soc.* **1960**, *82*, 3491–3495. (b) Jiang, P.; Guo, Z. *Coord. Chem. Rev.* **2004**, *248*, 205–229. (c) de Silva, A. P.; Gunaratne, H. Q. N.; Gunnlaugsson, T.; Huxley, A. J. M.; McCoy, C. P.; Rademacher, J. T.; Rice, T. E. *Chem. Rev.* **1997**, *97*, 1515–1566. (d) Ghosh, K.; Sen, T. *Beilstein J. Org. Chem.* **2010**, *6* (44), 8. (e) Kang, J.; Choi, M.; Kwon, J. Y.; Lee, E. Y.; Yoon, J. *J. Org. Chem.* **2002**, *67*, 4384–4386.

(20) (a) Choi, M.-Y.; Chan, M. C.-W.; Zhang, S.; Cheung, K.-K.; Che, C.-M.; Wong, K.-Y. *Organometallics* **1999**, *18*, 2074–2080. (b) Villata, L. S.; Wolcan, E.; Feliz, M. R.; Capparelli, A. L. *J. Phys. Chem. A* **1999**, *103*, 5661–5666. (c) Toyama, N.; Asano-Someda, M.; Ichino, T.; Kaizu, Y. *J. Phys. Chem. A* **2000**, *104*, 4857–4865. (d) Kaur, S.; Kumar, S. *Tetrahedron Lett.* **2004**, *45*, 5081–5085.

(21) (a) Ford, P.; Ogler, A. *Acc. Chem. Res.* **1993**, *26*, 220–226. (b) Bhardwaj, V. K.; Singh Pannu, A. P.; Singh, N.; Hundal, M. S.; Hundal, G. *Tetrahedron* **2008**, *64*, 5384–5391. (c) Xu, Z.; Zheng, S.; Yoon, J.; Spring, D. R. *Analyst* **2010**, *135*, 2554–2559. (d) Xu, Z.; Han, S. J.; Lee, C.; Yoon, J.; Spring, D. R. *Chem. Commun.* **2010**, *46*, 1679–1681. (e) Sheng, X.; Wei, L.; Kong-Chang, C. *Chin. J. Chem.* **2007**, *25*, 778–783.

(22) (a) Mashraqui, S. H.; Khan, T.; Sundaram, S.; Betkar, R.; Chandiramani, M. *Tetrahedron Lett.* **2007**, *48*, 8487–8490. (b) Connors, K. A. *Binding Constants*; Wiley: New York, 1987.

(23) (a) Salazar-Mendoza, D.; Baudron, S. A.; Hosseini, M. W. *Chem. Commun.* **2007**, 2252–2254. (b) Lahtinen, T.; Wegelius, E.; Rissanen, K. *New J. Chem.* **2001**, *25*, 905–911.

(24) (a) Kumar, S.; Luxami, V.; Saini, R.; Kaur, D. *Chem. Commun.* **2009**, 3044–3046. (b) Kumar, M.; Dhir, A.; Bhalla, V. *Org. Lett.* **2009**, *11*, 2567–2570. (c) Kumar, M.; Kumar, R. A.; Bhalla, V. *Chem. Commun.* **2009**, 7384–7386.

(25) (a) Khatua, S.; Choi, S. H.; Lee, J.; Huh, J. O.; Do, Y.; Churchill, D. G. *Inorg. Chem.* **2009**, *48*, 1799–1801. (b) Buncic, G.; Donnelly, P. S.; Paterson, B. M.; White, J. M.; Zimmermann, M.; Xiao, Z.; Wedd, A. G. *Inorg. Chem.* **2010**, *49*, 3071–3073.